



Published in final edited form as:

*J Alzheimers Dis.* 2017 ; 56(4): 1469–1484. doi:10.3233/JAD-160869.

## Treadmill Exercise Exerts Neuroprotection and Regulates Microglial Polarization and Oxidative Stress in a Streptozotocin-Induced Rat Model of Sporadic Alzheimer's Disease

Yujiao Lu, Yan Dong, Donovan Tucker, Ruimin Wang, Mohammad Ejaz Ahmed, Darrell Brann\*, and Quanguang Zhang\*

Department of Neuroscience and Regenerative Medicine, Medical College of Georgia, Augusta University, Augusta, GA, USA

### Abstract

Recent work has suggested that exercise may be beneficial in preventing or ameliorating symptoms of several neurological disorders, although the mechanism is not entirely understood. The current study was designed to examine the potential beneficial effect of treadmill exercise upon cognitive function in a streptozotocin (STZ)-induced rat model of Alzheimer's disease (AD). Animals underwent treadmill exercise (30 min/day, 5 days/week) for 4 weeks after bilateral STZ intracerebroventricular injection (2.4 mg/kg). We demonstrated that treadmill exercise significantly attenuated STZ-induced neurodegeneration in the rat hippocampal CA1 region and strongly preserved hippocampal-dependent cognitive functioning. Further mechanistic investigation displayed a marked suppression of STZ-induced amyloid- $\beta$  accumulation and tau phosphorylation. Intriguingly, treadmill exercise remarkably inhibited reactive gliosis following STZ insult and effectively shifted activated microglia from a pro-inflammatory M1 to an anti-inflammatory M2 phenotype, which was correlated with a significantly reduced expression of pro-inflammatory mediators and a corresponding enhancement of anti-inflammatory cytokine expression in the hippocampus. Furthermore, treadmill exercise caused a robust suppression of oxidative damage as evidenced by significantly reduced peroxynitrite production, lipid peroxidation, and oxidized DNA damage. Finally, treadmill exercise strongly attenuated STZ-induced mitochondrial dysfunction manifested by a dramatically elevated intra-mitochondrial cytochrome c oxidase activity and ATP synthesis, and markedly inhibited neuronal apoptosis in the hippocampus. These findings demonstrate that treadmill exercise has a multifactorial effect to attenuate many of the pathological processes that play a key role in AD, and provide further support for the beneficial role of exercise as a potential therapeutic option in AD treatment.

### Keywords

Alzheimer's disease; cognition; exercise; inflammation; microglia; oxidative stress; streptozotocin

---

\*Correspondence to: Dr. Quanguang Zhang, Associate Professor, Department of Neuroscience and Regenerative Medicine, Augusta University, 1120 15th Street, Augusta, GA 30912, USA. Tel.: +1 706 721 7025; Fax: +1 706 721 8685; qzhang@augusta.edu and Dr. Darrell W. Brann, Regents' Professor and Vice Chair, Department of Neuroscience and Regenerative Medicine, Augusta University, 1120 15th Street, CA-4004, Augusta, GA 30912, USA. Tel.: +706 721 7779; Fax: +1 706 721 8685; dbrann@augusta.edu.

## INTRODUCTION

Alzheimer's disease (AD) is the most common form of dementia in the elderly population, and leads to irreversible learning and cognitive deficits [1]. Extracellular amyloid- $\beta$  (A $\beta$ ) aggregation and intracellular neurofibrillary tangles are well known hallmarks of AD. Furthermore, the pathogenesis of AD is believed to be closely associated with a series of neurodegenerative events in the hippocampus, including microglial activation, neuroinflammation, oxidative stress, metabolic energy failure, and consequent neuronal apoptosis [2–7].

Neuroinflammation in AD is characterized by glial activation and release of inflammatory mediators, which triggers a vicious cycle of neuroinflammatory attack [8]. As the first line of defense against brain injuries, microglia are highly plastic cells that assume diverse phenotypes in response to specific signals from the microenvironment [9]. Two major phenotypes have been proposed for activated microglia: 1) a “classically activated” M1 “proinflammatory” phenotype that releases destructive proinflammatory mediators (e.g., IL-1 $\beta$ , IL-6, TNF- $\alpha$ ), and 2) a “selectively activated” M2 “repair/anti-inflammatory” phenotype which secretes neuroprotective, anti-inflammatory factors (e.g., IL-4 and IL-10) [10,11]. Interestingly, divergent roles for M1 and M2 polarized microglia have been reported in several neurodegenerative diseases, including AD, stroke, and spinal cord injury [9, 12–14], which raises the possibility that modulation of microglial phenotype could yield translational benefits in these neurodegenerative disorders.

In addition to a role for neuroinflammation, there is compelling evidence that oxidative stress plays an important pathogenic role in AD [15–17]. Oxidative stress causes irreversible damage to biological systems by oxidizing most of the cell's major biomolecules, including nucleic acid (DNA, RNA), protein, and lipids. The brain is particularly vulnerable to oxidative damage, as it possesses: 1) an abundance of easily peroxidized polyunsaturated fatty acids, 2) a high level of reactive oxygen species (ROS) and the catalyst iron, and 3) a relative paucity of antioxidant capacity [18]. In fact, oxidative imbalance leading to a buildup of damaging oxidative byproducts has been consistently reported in AD progression, even at the early stage before significant senile plaques have formed [19–21]. Furthermore, ROS accumulation in mitochondria causes a subsequent destruction of the electron transfer chain that leads to metabolic energy failure and mitochondrial dysfunction [22–24], which have a well-documented role in AD pathology [25, 26].

Streptozotocin (STZ) is a drug that upon peripheral injection selectively damages pancreatic  $\beta$ -cells, and thus has been widely used to generate an animal model for diabetes research [27, 28]. Intriguingly, a number of studies have also demonstrated that intracerebroventricular (ICV) injection of STZ into the brain of rodents induces AD-like pathology. For instance, ICV STZ induces progressive neuroinflammation, oxidative stress, and mitochondrial dysfunction, as well as marked A $\beta$  deposition and hyperphosphorylation of tau in the hippocampus; effects that are associated with significant learning and cognitive impairments [29–31]. The pathophysiological similarity in the effects of ICV injection of STZ in animals, and the pathology observed in AD patients, has led to the ICV STZ model being used extensively as a rodent experimental model for sporadic AD study [32–35].

While various drugs have been developed and utilized for AD treatment, they have only modest effects and significant side effects that unfortunately are common with many drug-based therapies. Recent studies have thus focused on identifying non-drug based therapies that may yield benefit in AD. One such non-drug based therapy that has received interest is running exercise. Exercise is known to increase the supply of both oxygen and nutrition to brain cells, as well as enhance the clearance of bodily wastes and carbon dioxide [36]. Intriguingly, exercise has been reported to induce neuronal and cerebrovascular proliferation, along with a markedly reduced accumulation of neurofibrillary tangles in AD animal models [37–40]. While a number of studies have confirmed the beneficial effect of exercise on AD, its effect upon neuroinflammation and oxidative stress, two key pathological processes during AD progression, has not been examined in detail. Also unclear is whether exercise might contribute to enhanced repair and decreased inflammatory damage in the AD brain by promoting activation of the M2 “repair” microglial phenotype.

To address these deficits in our understanding, the present study was designed to analyze the effect of treadmill exercise on neuroinflammatory and oxidative stress responses in the hippocampus using an STZ-induced rat model of AD. The effect of exercise on microglia polarization in the hippocampus was also assessed in the STZ model. The results of the study reveal that treadmill exercise causes a profound suppression of neuroinflammation and oxidative stress in the hippocampus after AD induction in the STZ model. Treadmill exercise also caused a robust enhancement of the M2 “repair/anti-inflammatory” microglial phenotype, with a corresponding suppression of the “proinflammatory” M1 phenotype in the hippocampus of the STZ-induced AD rat. These effects correlated with a profound reduction of neuronal apoptosis and significantly improved cognitive outcome.

## MATERIALS AND METHODS

### Animals and drug administration

Male Sprague Dawley rats (250–280 g, Charles River Laboratories) were used in this study. The rats were maintained at an ambient temperature of 22–24°C and 50–60% humidity, under a 12 h light: 12 h dark cycle. The animals were randomly divided into four groups: (1) normal control group with vehicle injection, (2) normal control group subjected to treadmill exercise, (3) STZ injection group, and (4) STZ injection plus treadmill exercise group. All animal studies were approved by, and conducted in accordance with the guidelines of the Institutional Animal Care and Use Committee of Augusta University. Behavioral tests to assess hippocampal function were carried out after treadmill exercise at six weeks after STZ injection. The animals were then sacrificed under deep anesthesia 51 days after STZ injection, and the brains were collected for immunofluorescent staining, western blot, and biochemical analyses. Bilateral ICV injection of STZ was carried out according to a previous study [41]. Briefly, STZ powder (Cayman Chemical Company) was dissolved in 0.9% sterile saline, and diluted to a concentration of 30 µg/µl. For ICV injection of STZ, rats were anesthetized with sodium pentobarbital (50 mg/kg, i.p.) and mounted in a stereotaxic apparatus. STZ (2.4 mg/kg) was bilaterally injected at a rate of 0.5 µl/min using a Hamilton microsyringe to the coordinates targeting cerebral ventricles (posterior: –0.8 mm, lateral: ±1.5 mm, depth: –3.5 mm). The needle was left *in situ* for 5 min before retraction, and then

retracted over 2 min. The incision was sterilized and closed, and the rats were placed on a warming pad to recover from anesthesia.

### **Treadmill exercise (Exe)**

Treadmill exercise was performed 1 week after ICV STZ treatment as previously described with little modification [42]. Briefly, one week of adaptive training was carried out in advance by cumulative intensity with a starting exercise of 2 m/min for 5 min, and then 5 m/min for 5 min, and finally 8 m/min for 20 min. The exercise regimen was then progressed to 8 m/min for 5 min, and then 14 m/min for 5 min, and finally to 18 m/min for 20 min. This main exercise regimen was subsequently performed for 5 days a week (for a total of 4 weeks). Correspondingly, rats from control groups were left on the treadmill without running for the same time.

### **Brain preparation and histological analysis**

Histological examination was performed by NeuN, F-Jade C, and TUNEL staining as described previously [43]. Briefly, after behavioral tests, the animals were transcardially perfused with ice-cold saline under deep anesthesia. The animals were then sacrificed by decapitation and the brain was quickly removed from the cranium and placed on an ice pack. The cerebral hemispheres were then separated along the longitudinal cerebral fissure. The hippocampus was rapidly microdissected from the right half of the brain along the hippocampal fissure and immediately frozen in liquid nitrogen until analysis. The left half of the brain hemisphere was postfixed in 4% paraformaldehyde at 4°C for 48 h, and cryoprotected with 30% sucrose for slices. Frozen-sections (20 µm) were cut on a Leica Rm2155 microtome in the coronal plane of the dorsal hippocampus (~2.5–4.5 mm posterior from Bregma). Every fifth section was saved in stock solution for required staining. Staining for NeuN and F-Jade C was performed using a mouse anti-NeuN monoclonal antibody (1:500; EMD Millipore) and F-Jade C (AG310; EMD Millipore) as described in detail by our laboratory [44]. NeuN-positive cells with intact and round nuclei, and negatively stained with F-Jade C, were counted as surviving cells. TUNEL staining was performed using the ApopTag® Plus Fluorescein *In Situ* Apoptosis Detection Kit (Chemicon) according to the manufacturer's instructions. All the images were captured on a Carl Zeiss LSM510 Meta confocal laser microscope as described [44]. For quantitative analyses, the number of F-Jade C, NeuN and TUNEL-positive cells per 250 µm length of hippocampus region were counted bilaterally in 3–5 representative sections per animal. Cell counts from the right and left hippocampus were averaged to provide a single value for each animal.

### **Brain homogenates and subcellular fractionation**

Hippocampal tissues were homogenized as described previously by our laboratory [45]. Briefly, homogenization was performed using a motor-driven Teflon homogenizer in 1 ml ice-cold homogenization buffer (50 mM HEPES, pH 7.4, 150 mM NaCl, 12 mM β-glycerophosphate, 1% Triton X-100) with inhibitors of proteases and enzymes (Thermo Scientific, Rockford, IL). The homogenates were vigorously mixed for 20 min on a rotator and centrifuged at 15,000 × g for 30 min at 4°C to obtain total protein fractions in the supernatants. For sub-cellular fractionation, tissues were homogenized in ice-cold buffer containing 10 mM HEPES (pH 7.9), 12 mM β-glycerophosphate, and inhibitors of proteases

and enzymes. After adding NP-40 to 0.6%, the homogenates were allowed to sit on ice for 10 min and vigorously vortexed for 30 s. The homogenates were then centrifuged at 800×g at 4°C for 10 min, and the pellets were discarded. The resulting supernatants were further centrifuged at 17,000 × g for 20 min at 4°C to yield crude mitochondrial fractions in the pellets and cytosolic fractions in the supernatants. Protein concentrations were determined via Modified Lowry Protein Assay (Pierce, Rockford, IL), and samples were aliquoted and stored at –80°C until use.

### Western blotting analysis

Western blotting was performed as previously described by our laboratory [45]. Primary antibodies we used were as follows: amyloid precursor protein C-Terminal from Sigma-Aldrich; PHF1 and Tau from Thermo Fisher; CD32, CD86, iNOS, ARG1, TGF-β, CD206 from Proteintech Group; 3-NT and β-actin from Santa Cruz. Proteins were transferred to PVDF membrane, blocked, and incubated with primary antibody at 4°C overnight. The membrane was then washed, followed by incubation with HRP-conjugated secondary antibodies for 1 h at room temperature. Bound proteins were visualized using a CCD digital imaging system, and semi-quantitative analyses of the bands were performed with the ImageJ analysis software (Version 1.49; NIH, USA). Band densities for the indicated proteins were normalized to loading controls.

### Immunofluorescence staining and confocal microscopy

As previously described [43], brain floating sections were incubated with 10% normal donkey serum for 1 h at room temperature, followed by incubation with appropriate primary antibodies overnight. The following primary antibodies were used in different combinations: anti-NeuN (MAB377, Millipore); anti-Aβ<sub>42</sub> and anti-PHF1 (Thermo Fisher); anti-IBA1 (Proteintech Group); anti-P-H2A.X (Cell Signaling); anti-4-HNE and anti-8-OHdG (Abcam Inc.). Sections were then washed four times at room temperature, followed by incubation with proper Alexa Fluor 594/488 donkey anti-mouse/rabbit secondary antibody (Thermo Fisher) for 1 h. After washes, sections were mounted and coverslipped in Vectashield mounting medium with DAPI (Vector Laboratories). All the fluorescence images were captured on an LSM510 Meta confocal laser microscope (Carl Zeiss) using 40×oil immersion Neofluor objectives with the image size set at 1024 x 1024 pixels. The captured images were viewed and analyzed using LSM510 Meta imaging software. At least 4–5 representative sections per animal were utilized for immunostaining and the typical staining was selected for presentation.

### Measurement of Aβ<sub>1–42</sub> levels

The levels of Aβ<sub>1–42</sub> in each group were detected using an Aβ<sub>1–42</sub> ELISA Kit (Catalog # KMB3441, Thermo Fisher) in accordance with the manufacturer's instruction. Detergent-soluble Aβ<sub>1–42</sub> level was detected in protein samples that were collected as described above. Detergent-insoluble Aβ<sub>1–42</sub> content was examined by extraction of homogenate pellets in 5 M guanidine-HCl. Briefly, equal amounts of protein in each group were diluted to 100 μl volume and incubated in plate wells at room temperature for 2 h. The plate wells were then washed and incubated with 100 μl of Detection Antibody solution for 1 h at room temperature. Afterwards, the wells were washed and incubated with 100 μl of HRP-linked

antibody solution for 30 min followed by 4 times of wash. Finally, the optical density was read at 450 nm on a spectrophotometer (Bio-Rad) after the adding of Stop Solution. A $\beta$ <sub>1-42</sub> levels were calculated and expressed as percent change versus control group.

### **Quantification of ATP levels and cytochrome C oxidase (CCO) activity**

As previously described [46], ATP concentrations were detected using an ENLITEN<sup>®</sup> rLuciferase/Luciferin reagent kit (FF2021, Promega) following the manufacturer's instructions. Briefly, 30  $\mu$ g of sample proteins from total protein fractions were suspended in 100  $\mu$ l of reconstituted rL/L reagent buffer. Light emission at 10 s intervals from the reaction was measured in a standard microplate luminometer (PE Applied Biosystems). Relative light units (RLU) from rL/L reagent and the homogenization buffer used to prepare the samples were subtracted from the reaction assay. An ATP standard curve was used to determine levels of ATP activity. The mitochondrial fraction was used to assess CCO activity with an ATP activity assay kit (ab109911, Abcam Inc.), according to the manufacturer's instructions. CCO enzyme was immunocaptured within the 96-well microplate, and activity was evaluated by measuring the oxidation of Cytochrome C at 550 nm absorbance (Bio-Rad Benchmark Plus). The values of ATP levels and relative CCO activity were expressed as percentage change versus control group.

### **Inflammatory cytokine assays**

The levels of pro-inflammatory cytokines (IL-1 $\beta$ , TNF- $\alpha$ ) and anti-inflammatory cytokines (IL-4, IL-10) were quantitatively detected by the indirect ELISA technique [47]. Briefly, 50  $\mu$ L of protein samples containing the same amount of proteins were prepared using bicarbonate/carbonate coating buffer (Sigma-Aldrich). Samples were loaded in a PVC ELISA microplate (Corning), sealed, and incubated overnight at 4°C. After four washes, the remaining protein-binding sites in the coated wells were blocked by adding 200  $\mu$ L blocking buffer (1% BSA in PBS, 0.3% solution of H<sub>2</sub>O<sub>2</sub>) for 1 h at room temperature. Afterwards, 50  $\mu$ L of specific antibodies were added and incubated for 4 h at 37°C. The plate wells were then washed and incubated with HRP-conjugated secondary antibodies for 1 h at room temperature. Finally, the plate was washed and developed by incubating with TMB (3,3', 5,5'-tetramethylbenzidine) solution (Thermo Fisher) for 30 min, and the reaction was stopped with 50  $\mu$ L of sulfuric acid. The plate wells were then read at 450 nm on a spectrophotometer (Bio-Rad), and values were calculated and expressed as percent change versus control group.

### **Caspase activity assay**

Caspase-3 and caspase-9 activities in the cytosolic protein fractions were measured using fluorometric substrates as previously described [46]. The Ac-DEVD-AMC and Ac-LEHD-AMC (AnaSpec) are substrates for caspase-3 and caspase-9, respectively. The fluorescence of free AMC was determined with an excitation wavelength of 360 nm and an emission wavelength of 460 nm, in a Synergy HT Microplate reader (BioTek Instruments). The values were expressed as fold change in fluorescent units compared with control group.



### **Barnes maze task**

The Barnes Maze task is used to test hippocampus-dependent spatial learning and memory [48, 49], and was adopted by our laboratory as previously described [46]. The traces of rats were monitored by an overhead video camera controlled by ANY-maze video tracking software (Stoelting Co., Wood Dale, IL). Briefly, on day 43, 44, and 45 after STZ injection, 3 days of training trials were performed with a maximum trial length of 180 s. On each trial day, escape latency of rat from the platform center to the escape chamber was recorded. The probe trial was performed on day 46 after STZ injection. The escape box was removed, and time spent in the target quadrant where the escape box had been was recorded for 90 s. The platform was cleaned with 70% ethanol and dried with a blower fan after each test. Searching error was defined as exploring any hole that did not have target chamber under it. The quadrant occupancy and numbers of errors were quantified afterwards using ANY-maze software.

### **Passive avoidance test**

The passive avoidance test was performed as described previously [50]. The apparatus employed in this test consisted of two compartments, one bright and one dark, separated by a vertical sliding door. The test was divided into two stages. In stage one, on day 47 after STZ injection, rat was put in the bright compartment for 20-s habituation, after which the door was opened and the rat was allowed to enter the dark compartment. Once the rat entered the dark compartment, the door was closed, leaving the rat in the dark room for 20 s. The rat was then given a 0.3 mA electric shock for 2 s. After a 10-s recovery period, the rat was returned to its home cages. In stage two, 24 h after being returned to the home cage the rat was put in the bright room again for 20 s with the door closed. Afterwards, the door was opened, and the latency time for rat stepping through the door and the numbers of rats from each group staying in the bright chamber over 300 s were recorded.

### **Novel object recognition test**

The novel object recognition test was used to evaluate the effects of treadmill exercise on the functional improvement in recognition memory, a hippocampus-dependent working memory in rats [49, 51]. The novel object recognition test is based on the spontaneous tendency of rats to spend more time exploring a novel object than a familiar object. The test was divided into three stages. In stage one, on day 49 after STZ injection, the rat was allowed 5 min to explore an empty recognition box (40×50×50 cm) for habituation. In stage two, 24 h later, the rat was placed in the same recognition box containing two identical objects at an equal distance for 5-min exploration. In stage three, 48 h later, the rat was returned to the object recognition box in presence of one familiar object and one novel object to test long-term recognition memory. The novel object is generally consistent in height and volume with the familiar object, but is different in shape and appearance. Exploration of the object was defined as the animal's nose being in a zone within 2 cm from the object. The time spent exploring each object and the discrimination index percentage (the percentage time spent exploring the new object) were recorded and analyzed using ANY-maze video tracking software as described above.

## Data analysis

Statistical analysis was performed using one-way analysis of variance (ANOVA) or two-way, ANOVA followed by Student-Newman-Keuls *post-hoc* tests to determine group differences. When groups were compared to the normal control group, Dunnett's test was adopted for *post-hoc* analyses after ANOVA. When only two groups were compared, a Student's *T* test was used. Statistical significance was accepted at the 95% confidence level ( $p < 0.05$ ). Data were expressed as means  $\pm$  SE.

## RESULTS

### Treadmill exercise alleviates STZ-induced cognitive deficits in the Barnes maze task, passive avoidance test, and novel object recognition test

To investigate the effect of treadmill exercise on preserving spatial learning and memory function following ICV STZ injection, we utilized the Barnes maze task, a commonly applied test of hippocampus-dependent spatial reference learning and memory in rats [48, 49]. As shown in Fig. 1A and B, Barnes maze results revealed that STZ-injected rats had a significant increase in latency to find the hidden chamber in training trials and a decrease in quadrant occupancy on probe day, as compared to control rats. Interestingly, animals that underwent treadmill exercise displayed remarkable cognitive improvement compared with the STZ group, as evidenced by exercise rats exhibiting a marked decrease in escape latency to find the chamber and a notable elevation in quadrant occupancy. It should be noted that there was no significant difference in escape velocity among the groups, suggesting that differences in escape latencies were not due to speed variations among different groups. Further examination revealed that STZ rats also had a significant elevation of exploration errors on probe day, as compared to the control group, and this effect was significantly reversed by treadmill exercise. As an alternative method to examine impaired cognitive function after STZ insult, we performed the passive avoidance test and recorded both step-through latency and numbers of rats staying in the light over 300 s (Fig. 1C). The results revealed that STZ-injected rats had significantly impaired memory function with decreased latency to enter the dark room, and this effect was significantly reversed by treadmill exercise. The number of treadmill exercise rats that remained in the lit chamber room over 300 s was significantly greater than the number of STZ-injected rats. To determine whether treadmill exercise could preserve recognition memory in STZ-injected rats, we performed a novel object recognition test [51]. As shown in Fig. 1D, STZ-injected rats had an impaired recognition memory, as evidenced by a decreased preference to explore the novel object as compared with normal control. In contrast, animals that underwent treadmill exercise had enhanced preference for novel object exploration. Intriguingly, we did not observe a significant memory change between the non-STZ-treated control group and the non-STZ-treated control group plus treadmill exercise in any of the behavioral tests (data not shown), indicating that 4 weeks' treadmill exercise does not significantly alter the memory functions in normal control rats.

### Treadmill exercise attenuates STZ-induced hippocampal neuronal degeneration

To examine the efficacy of treadmill exercise on STZ-induced hippocampal neuronal degeneration, we collected hippocampal CA1 region sections and stained them using a



neuron-specific marker (NeuN) and a marker of neuronal degeneration (F-Jade C). As shown in Fig. 2A, CA1 pyramidal neurons from rats subjected to STZ administration exhibited a significant loss of Neu-N positive neuronal cells, and exhibited robust neuronal degeneration as evidenced by a significantly higher level of F-Jade C staining, as compared with normal controls. In contrast, treadmill exercise markedly reduced the STZ-induced neuronal degeneration as evidenced by a marked reduction in F-Jade C in the hippocampal CA1 region, as compared to the STZ-injected animals. Quantification analysis of NeuN-positive “surviving” neurons and F-Jade C positive degenerating neurons was subsequently performed, and confirmed that STZ infusion resulted in 50% neuronal loss and a significant elevation in F-Jade C positive neurons, effects that were significantly reversed by treadmill exercise (Fig. 2B).

### **Treadmill exercise inhibits elevation of amyloidogenic processing and hyperphosphorylation of tau protein in the hippocampal CA1 region of STZ rats**

To determine the effect of treadmill exercise on non-amyloidogenic and amyloidogenic pathways of amyloid- $\beta$  protein precursor (A $\beta$ PP) processing, we examined the C-99/C-83 ratio in the hippocampal CA1 region from different groups. In the non-amyloidogenic pathway of A $\beta$ PP processing, cleavage by  $\alpha$ -secretase within the amyloid- $\beta$  domain yields a soluble amyloid- $\beta$  protein precursor fragment (sA $\beta$ PP $\alpha$ ) and a C-terminal fragment (C-83), and thus precludes A $\beta$  deposit. However, in the amyloidogenic pathway of A $\beta$ PP cleavage, cleavage of A $\beta$ PP by  $\beta$ -secretase (BACE1) yields an N-terminal soluble domain with a membrane-tethered C-terminal domain (C-99), and A $\beta$ <sub>1-42</sub> is subsequently released by  $\gamma$ -secretase cleavage within the transmembrane domain of A $\beta$ . Examination of the C-99/C-83 ratio in our study revealed that rats subjected to STZ injection had an enhanced C-99/C-83 A $\beta$ PP ratio in the hippocampal CA1 region, which is indicative of active induction of the amyloidogenic pathway. In contrast, rats undergoing treadmill exercise showed a significant reduction in the C-99/C-83 ratio, suggesting an inhibited A $\beta$ PP amyloidogenic processing (Fig. 3A). We next wanted to confirm that enhanced amyloidogenic processing of A $\beta$ PP led to elevated A $\beta$  generation. A specific A $\beta$ <sub>1-42</sub> ELISA was used to investigate the content of intra-neuronal detergent soluble (Fig. 3B) and extracellular detergent-insoluble A $\beta$ <sub>1-42</sub> (Fig. 3C). The results showed a significant increase for both intraneuronal A $\beta$  and extraneuronal oligomers in the hippocampal CA1 region of the STZ-injected rats, an effect that was markedly attenuated by treadmill exercise. To further confirm the suppressive effect of treadmill exercise on A $\beta$  generation, A $\beta$ <sub>1-42</sub> immunofluorescent staining was carried out. As shown in Fig. 3D, representative confocal images of A $\beta$ <sub>1-42</sub> staining revealed elevated A $\beta$  formation in the hippocampal CA1 region in STZ-injected rats, as compared to control. In contrast, treadmill exercise significantly suppressed the robust A $\beta$  generation, as evidenced by decreased A $\beta$  staining. We next used staining of hippocampal CA1 region sections with a specific anti-PHF1 antibody to examine another key hallmark of AD, hyperphosphorylation of tau protein. As shown in Fig. 3E, STZ-injected rats exhibited a significant increase in hyperphosphorylated tau staining in the hippocampal CA1 region, as compared to controls. In contrast, treadmill exercise significantly attenuated hyperphosphorylation of tau in the STZ-injected rats. Finally, western blot analysis further confirmed the increase of tau hyperphosphorylation in the hippocampal CA1 region of STZ-injected rats, and the attenuating effect of treadmill exercise (Fig. 3F).

### **Treadmill exercise shifts microglial polarization to the M2 “repair/anti-inflammatory” phenotype and suppresses the production of pro-inflammatory cytokines**

Previous work has shown that reactive gliosis is induced concurrent with elevated oligomeric A $\beta$  species and plays an important role in AD pathology [49]. Therefore, we next examined the effect of treadmill exercise upon microgliosis and microglial polarization in the hippocampal CA1 region of STZ-injected rats. Representative confocal images of hippocampal CA1 region sections stained with the microglial marker, IBA1, revealed that STZ rats had a significant increase in microgliosis, and this effect was reversed by treadmill exercise (Fig. 4A). According to previous studies, activated microglia can be polarized to divergent M1 or M2 phenotypes and secrete corresponding pro-inflammatory or anti-inflammatory cytokines in neurodegenerative disorders as a result of the particular *in vivo* microenvironment. Western blot analysis was thus performed for M1 and M2 markers to determine microglia polarization in the hippocampal CA1 region of STZ rats and the effect of exercise. As shown in Fig. 4B, western blot analysis of representative M1 markers (CD32, CD86, iNOS) in total protein samples from hippocampal CA1 region showed that STZ injection caused a significant increase in all three M1 marker proteins, as compared with normal control, suggesting that the activated microglia were polarized predominantly to an M1 phenotype after STZ insult. In contrast, the elevation of all three M1 marker proteins was strongly attenuated in the treadmill exercise group. We next utilized western blot analysis to examine the effect of STZ injection and treadmill exercise upon protein expression levels of several M2 markers (ARG1, TGF- $\beta$ , CD206) in the hippocampal CA1 region. As shown in Fig. 4C, STZ injection had no significant effect upon any of the M2 marker protein levels, as compared to the control group. In contrast, treadmill exercise markedly elevated protein expression levels for all three M2 markers in the hippocampal CA1 region, as compared with STZ only group, suggesting treadmill exercise helps to shift activated microglia to a potentially more beneficial M2 “repair/anti-inflammatory” phenotype. To confirm that the change in M1/M2 microglia phenotype by treadmill exercise was actually correlated with a change in production of pro-inflammatory and anti-inflammatory cytokines, ELISA assays were used to measure the levels of specific pro-inflammatory cytokines (IL-1 $\beta$ , TNF- $\alpha$ ) and anti-inflammatory cytokines (IL-4 $\beta$ , IL-10 $\beta$ ) in the hippocampal CA1 region. As shown in Fig. 4D, the cytokine ELISA assays revealed a robust elevation of the pro-inflammatory cytokines IL-1 $\beta$  and TNF- $\alpha$ , and a significant decrease in anti-inflammatory cytokines IL-4 and IL-10 in STZ-injected rats, effects that were markedly reversed by treadmill exercise.

### **Treadmill exercise ameliorates STZ-induced oxidative stress damage to basic cellular components**

Oxidative stress has been well documented to cause oxidative damage to many cellular components in AD and other neurodegenerative disorders [43, 52–54]. We therefore sought to examine the effect of STZ injection and treadmill exercise upon oxidative damage in the hippocampal CA1 region using oxidative markers for peroxynitrite production (3-NT), lipid peroxidation (4-HNE), DNA double-strand breaks (P-H2A.X), and oxidized DNA damage (8-OHdG). As shown in Fig. 5A, western blot analysis showed a robust increase of 3-NT intensity in the hippocampal CA1 region of STZ rats, as compared to the control group. Interestingly, treadmill exercise significantly attenuated the STZ-induced increase of 3-NT

in the hippocampal CA1 region (Fig. 5B). Confocal microscopy and immunoreactivity examinations of 4-HNE, P-H2A.X, and 8-OHdG in the hippocampal CA1 region revealed enhanced immunostaining for these oxidative stress markers in STZ rats, and these effects were significantly reversed by treadmill exercise (Fig. 5B, C).

### **Treadmill exercise attenuates STZ-induced mitochondrial dysfunction and the consequent activation of caspase-9/caspase-3 apoptotic pathway**

Since neuroinflammation and oxidative stress can accelerate mitochondrial dysfunction and lead to energy metabolic failure, we thus investigated the function of the intra-mitochondrial electron transfer chain where ATP is synthesized. As shown in Fig. 6A and B, STZ infusion resulted in a significant decline in cytochrome c oxidase (CCO) activity that correlated with a robust reduction of ATP levels in the hippocampus, as compared with control animals. Of significant interest, treadmill exercise markedly enhanced CCO activity and ATP production, demonstrating the effective recovery of energy metabolism following endurance exercise. Furthermore, as shown in Fig. 6C and D, STZ induced a significant enhancement of the activity of the pro-apoptotic proteins, caspase 3 and 9, as determined by fluorometric substrate assay, and this effect was significantly attenuated by treadmill exercise. Finally, the effect of STZ and exercise upon apoptosis was explored by TUNEL staining of hippocampal CA1 sections. As shown in Fig. 6E and F, STZ induced a robust increase in TUNEL-positive cells, as compared with normal controls, and this effect was significantly reversed by treadmill exercise.

## **DISCUSSION**

Intracerebroventricular injection of STZ produces a series of pathological effects that resembles the features of sporadic AD, and thus has been widely employed as a non-transgenic model of preclinical investigation for AD treatment [41, 55, 56]. Using the STZ model of sporadic AD, the present study provided evidence that treadmill exercise yields significant hippocampal neuroprotection and cognitive preservation following ICV STZ injection. The neuroprotective and cognitive preserving effects of treadmill exercise are likely due to the multifactorial beneficial effects demonstrated in our study, which include a reduction of amyloidogenesis and tauopathy, suppression of neuroinflammation and oxidative stress, as well as preservation of energy metabolic function in the hippocampal CA1 region.

Of these different pathological events, the amyloid cascade has been long proposed as a key event that facilitates downstream pathophysiologic processes in AD that culminate in neurodegeneration and cognitive decline [49, 57, 58]. Indeed, accumulating evidence has shown that insulin affects both A $\beta$  deposit as well as tau phosphorylation by modulating the PI3K signaling pathway. For instance, Kang et al. recently reported that ICV-STZ administration in rats leads to remarkable A $\beta$  deposit in the brain, possibly via the suppression of insulin receptor and insulin receptor substrate, followed by Akt and GSK3 $\alpha$  inactivation, which was strongly reversed by 6 weeks of treadmill exercise [42]. CDK5 can also phosphorylate A $\beta$ PP and tau and is robustly activated during insulin signaling

disturbance [59]. However, despite its ability to activate PI3K signaling, treadmill exercise did not significantly inhibit CDK5 activity [60].

The human genetic evidence that any mutation in A $\beta$ PP leading to A $\beta$  aggregation invariably causes early-onset of AD strongly supports the amyloid cascade hypothesis [61]. In examining the effects of treadmill exercise on amyloidogenesis and tauopathy, the present study revealed a significantly elevated C-83/C-99 ratio and hyperphosphorylated tau levels in the hippocampal CA1 region following STZ insult, indicating active amyloidogenic pathway processing and active tauopathy in STZ rats, which was strongly inhibited by treadmill exercise. Interestingly, our study further confirmed that treadmill exercise caused a robust decrease in STZ-induced elevations of soluble and insoluble A $\beta$  levels in the hippocampus. In agreement with our results, Coreia et al. also found a significant increase in hippocampal A $\beta$ <sub>1-42</sub> and hyperphosphorylated tau levels 5 weeks after bilateral ICV STZ injection (3 mg/kg) [62], although their study did not examine the effects of exercise.

Interestingly, elevation of soluble and oligomeric A $\beta$  species is well known to be associated with induction of reactive gliosis and neuroinflammation during AD progression [63]. In agreement, we found that STZ rats had a significant increase in activated microglia after STZ injection, which was strongly reversed by treadmill exercise. A novel finding of our study was that treadmill exercise induced a potentially beneficial change in microglial polarization in the STZ animal model of sporadic AD. Along these lines, treadmill exercise was found to suppress the STZ-induced M1 “pro-inflammatory” microglia phenotype, and enhance the M2 “repair/anti-inflammatory” microglia phenotype in the hippocampal CA1 region. To our knowledge this is the first report of treadmill exercise exerting a beneficial regulation of microglial phenotype in an AD animal model. Furthermore, the decrease in M1 and enhancement of M2 microglia phenotype by treadmill exercise was associated with a parallel decrease in secretion of pro-inflammatory cytokines, and enhanced production of anti-inflammatory cytokines. This modulation of the cytokine profile of the microglia is likely to contribute to lowered inflammatory damage and increased repair of brain cells, which may underlie, in part, the overall beneficial effects of exercise on neurodegeneration and cognitive function. In support of this possibility, recent work has shown that transplantation of M2 microglia in the brain resulted in reduced neuroinflammation and improved cognitive function in an A $\beta$ -treated rat model of AD [64].

In addition to regulation of microglial polarization, our study demonstrated that treadmill exercise exerts powerful anti-oxidative stress effects in the hippocampus of STZ rats to suppress oxidative damage to lipids, proteins, and nucleic acids. The anti-oxidative stress effects of treadmill exercise also likely contribute to the exercise-induced neuroprotection and cognitive improvement observed in this study. Furthermore, oxidative stress is well accepted as a key pathological event that contributes to AD pathogenesis, and is closely linked to induction of neuroinflammation in AD [65–68]. For instance, a number of studies have found that increased ROS accumulation within mitochondria can feedback and facilitate mitochondrial dysfunction, leading to structural damage to the electron transfer chain and resultant ATP synthesis failure [69–71]. In fact, impaired oxidative phosphorylation and decreased ATP generation have been observed in the brains of AD patients, and is viewed as a sensitive index for monitoring cognitive alteration in AD

progression [72–74]. It is thus of significant interest that in our study, treadmill exercise reversed STZ-induced reduction of cytochrome c oxidase activity and subsequent ATP depletion in the hippocampal CA1 region. Furthermore, it is well known that neurons in the brain can undergo apoptosis due to increased oxidative damage, neuroinflammation, and metabolic energy failure. In support of this, our study found that STZ rats displayed robust activation of pro-apoptotic proteins caspase 3 and caspase 9, and a corresponding increased number of TUNEL-positive cells in the hippocampus. Treadmill exercise had a strong anti-apoptotic effect as evidenced by its ability to suppress the STZ induction of the pro-apoptotic caspases and reduce the number of TUNEL-positive cells in the hippocampus.

The current study demonstrates that treadmill exercise exerts profound neuroprotective and cognitive preserving effects in an STZ-induced animal model of sporadic AD. Although the neuroprotective mechanism of treadmill exercise requires further study, the results of the current study suggests that the beneficial effects of treadmill exercise are due to a multifactorial effect to inhibit amyloidogenesis and tauopathy, suppress oxidative stress and neuroinflammation, and preserve metabolic energy function in the hippocampus. As a whole, these findings provide novel insights into the mechanisms underlying the beneficial effect of treadmill exercise in AD, and support further studies upon the therapeutic potential of exercise for preventing or ameliorating the devastating neurological consequences of AD.

## Acknowledgments

This research was supported by Research Grants (NS086929 and NS088058) from the National Institutes of Neurological Disorders and Stroke, National Institutes of Health, and an American Heart Association Grant-in-Aid (15GRNT25240004).

Authors' disclosures available online (<http://j-alz.com/manuscript-disclosures/16-0869r2>).

## References

1. Myhrer T. Neurotransmitter systems involved in learning and memory in the rat: A meta-analysis based on studies of four behavioral tasks. *Brain Res Brain Res Rev.* 2003; 41:268–287. [PubMed: 12663083]
2. Simonian NA, Coyle JT. Oxidative stress in neurodegenerative diseases. *Annu Rev Pharmacol Toxicol.* 1996; 36:83–106. [PubMed: 8725383]
3. Behl C, Holsboer F. Oxidative stress in the pathogenesis of Alzheimer's disease and antioxidant neuroprotection. *Fortschr Neurol Psychiatr.* 1998; 66:113–121. [PubMed: 9565761]
4. Koliatsos VE, Kecojevic A, Troncoso JC, Gastard MC, Bennett DA, Schneider JA. Early involvement of small inhibitory cortical interneurons in Alzheimer's disease. *Acta Neuropathol.* 2006; 112:147–162. [PubMed: 16758165]
5. Akama KT, Van Eldik LJ. Beta-amyloid stimulation of inducible nitric-oxide synthase in astrocytes is interleukin-1beta- and tumor necrosis factor-alpha (TNFalpha)-dependent, and involves a TNFalpha receptor-associated factor- and NFkappaB-inducing kinase-dependent signaling mechanism. *J Biol Chem.* 2000; 275:7918–7924. [PubMed: 10713108]
6. Behl C, Davis JB, Lesley R, Schubert D. Hydrogen peroxide mediates amyloid beta protein toxicity. *Cell.* 1994; 77:817–827. [PubMed: 8004671]
7. Griffin WS, Mrak RE. Interleukin-1 in the genesis and progression of and risk for development of neuronal degeneration in Alzheimer's disease. *J Leukoc Biol.* 2002; 72:233–238. [PubMed: 12149413]

8. Wilkins HM, Carl SM, Weber SG, Ramanujan SA, Festoff BW, Linseman DA, Swerdlow RH. Mitochondrial lysates induce inflammation and Alzheimer's disease-relevant changes in microglial and neuronal cells. *J Alzheimers Dis.* 2005; 45:305–318.
9. Kigerl KA, Gensel JC, Ankeny DP, Alexander JK, Donnelly DJ, Popovich PG. Identification of two distinct macrophage subsets with divergent effects causing either neurotoxicity or regeneration in the injured mouse spinal cord. *J Neurosci.* 2009; 29:13435–13444. [PubMed: 19864556]
10. Durafourt BA, Moore CS, Zammit DA, Johnson TA, Zaguia F, Guiot MC, Bar-Or A, Antel JP. Comparison of polarization properties of human adult microglia and blood-derived macrophages. *Glia.* 2012; 60:717–727. [PubMed: 22290798]
11. Goerdts S, Politz O, Schledzewski K, Birk R, Gratchev A, Guillot P, Hakiy N, Klemke CD, Dippel E, Kodolja V, Orfanos CE. Alternative versus classical activation of macrophages. *Pathobiology.* 1999; 67:222–226. [PubMed: 10725788]
12. Hu X, Li P, Guo Y, Wang H, Leak RK, Chen S, Gao Y, Chen J. Microglia/macrophage polarization dynamics reveal novel mechanism of injury expansion after focal cerebral ischemia. *Stroke.* 2012; 43:3063–3070. [PubMed: 22933588]
13. Zhu D, Yang N, Liu YY, Zheng J, Ji C, Zuo PP. M2 macrophage transplantation ameliorates cognitive dysfunction in amyloid- $\beta$ -treated rats through regulation of microglial polarization. *J Alzheimers Dis.* 2016; 52:483–495. [PubMed: 27003214]
14. Jiang T, Zhang YD, Chen Q, Gao Q, Zhu XC, Zhou JS, Shi JQ, Lu H, Tan L, Yu JT. TREM2 modifies microglial phenotype and provides neuroprotection in P301S tau transgenic mice. *Neuropharmacology.* 2016; 105:196–206. [PubMed: 26802771]
15. Moreira PI, Carvalho C, Zhu X, Smith MA, Perry G. Mitochondrial dysfunction is a trigger of Alzheimer's disease pathophysiology. *Biochim Biophys Acta.* 2010; 1802:2–10. [PubMed: 19853658]
16. Moreira PI, Duarte AI, Santos MS, Rego AC, Oliveira CR. An integrative view of the role of oxidative stress, mitochondria and insulin in Alzheimer's disease. *J Alzheimers Dis.* 2009; 16:741–761. [PubMed: 19387110]
17. von Bernhardi R, Eugenín-von Bernhardi L, Eugenín J. Microglial cell dysregulation in brain aging and neurodegeneration. *Front Aging Neurosci.* 2015; 7:124. [PubMed: 26257642]
18. Wang X, Wang W, Li L, Perry G, Lee HG, Zhu X. Oxidative stress and mitochondrial dysfunction in Alzheimer's disease. *Biochim Biophys Acta.* 2014; 1842:1240–1247. [PubMed: 24189435]
19. Mufson EJ, Chen EY, Cochran EJ, Beckett LA, Bennett DA, Kordower JH. Entorhinal cortex beta-amyloid load in individuals with mild cognitive impairment. *Exp Neurol.* 1999; 158:469–490. [PubMed: 10415154]
20. Markesbery WR, Schmitt FA, Kryscio RJ, Davis DG, Smith CD, Wekstein DR. Neuropathologic substrate of mild cognitive impairment. *Arch Neurol.* 2006; 63:38–46. [PubMed: 16401735]
21. Price JL, McKeel DW, Buckles VD, Roe CM, Xiong C, Grundman M, Hansen LA, Petersen RC, Parisi JE, Dickson DW, Smith CD, Davis DG, Schmitt FA, Markesbery WR, Kaye J, Kurlan R, Hulette C, Kurland BF, Higdon R, Kukull W, Morris JC. Neuropathology of nondemented aging: Presumptive evidence for preclinical Alzheimer disease. *Neurobiol Aging.* 2009; 30:1026–1036. [PubMed: 19376612]
22. Yamane T, Ikari Y, Nishio T, Ishii K, Ishii K, Kato T, Ito K, Silverman DH, Senda M, Asada T, Arai H, Sugishita M, Iwatsubo T. Study J-ADNI, Group. Visual-statistical interpretation of (18)F-FDG-PET images for characteristic Alzheimer patterns in a multicenter study: Inter-rater concordance and relationship to automated quantitative evaluation. *AJNR Am J Neuroradiol.* 2014; 35:244–249. [PubMed: 23907243]
23. Shokouhi S, Claassen D, Kang H, Ding Z, Rogers B, Mishra A, Riddle WR. Alzheimer's Disease Neuroimaging Initiative. Longitudinal progression of cognitive decline correlates with changes in the spatial pattern of brain 18F-FDG PET. *J Nucl Med.* 2013; 54:1564–1569. [PubMed: 23864720]
24. Landau SM, Harvey D, Madison CM, Koeppe RA, Reiman EM, Foster NL, Weiner MW, Jagust WJ. Alzheimer's Disease Neuroimaging Initiative. Associations between cognitive, functional, and FDG-PET measures of decline in AD and MCI. *Neurobiol Aging.* 2011; 32:1207–1218. [PubMed: 19660834]



25. de la Torre JC. Pathophysiology of neuronal energy crisis in Alzheimer's disease. *Neurodegener Dis.* 2008; 5:126–132. [PubMed: 18322369]
26. Parihar MS, Brewer GJ. Mitochondrial failure in Alzheimer disease. *Am J Physiol Cell Physiol.* 2007; 292:C8–23. [PubMed: 16807300]
27. Plaschke K, Hoyer S. Action of the diabetogenic drug streptozotocin on glycolytic and glycogenolytic metabolism in adult rat brain cortex and hippocampus. *Int J Dev Neurosci.* 1993; 11:477–483. [PubMed: 8237464]
28. Lester-Coll N, Rivera EJ, Soscia SJ, Doiron K, Wands JR, de la Monte SM. Intracerebral streptozotocin model of type 3 diabetes: Relevance to sporadic Alzheimer's disease. *J Alzheimers Dis.* 2006; 9:13–33. [PubMed: 16627931]
29. Hoyer S, Lannert H. Inhibition of the neuronal insulin receptor causes Alzheimer-like disturbances in oxidative/energy brain metabolism and in behavior in adult rats. *Ann N Y Acad Sci.* 1999; 893:301–303. [PubMed: 10672254]
30. Salkovic-Petrisic M, Hoyer S. Central insulin resistance as a trigger for sporadic Alzheimer-like pathology: An experimental approach. *J Neural Transm Suppl.* 2007; 72:217–233.
31. Grünblatt E, Salkovic-Petrisic M, Osmanovic J, Riederer P, Hoyer S. Brain insulin system dysfunction in streptozotocin intracerebroventricularly treated rats generates hyperphosphorylated tau protein. *J Neurochem.* 2007; 101:757–770. [PubMed: 17448147]
32. Agrawal R, Tyagi E, Shukla R, Nath C. A study of brain insulin receptors, AChE activity and oxidative stress in rat model of ICV STZ induced dementia. *Neuropharmacology.* 2009; 56:779–787. [PubMed: 19705549]
33. Ishrat T, Parveen K, Khan MM, Khuwaja G, Khan MB, Yousuf S, Ahmad A, Shrivastav P, Islam F. Selenium prevents cognitive decline and oxidative damage in rat model of streptozotocin-induced experimental dementia of Alzheimer's type. *Brain Res.* 2009; 1281:117–127. [PubMed: 19374888]
34. Santos DB, Colle D, Moreira EL, Peres KC, Ribeiro RP, dos Santos AA, de Oliveira J, Hort MA, de Bem AF, Farina M. Probucol mitigates streptozotocin-induced cognitive and biochemical changes in mice. *Neuroscience.* 2015; 284:590–600. [PubMed: 25453776]
35. Zhao SS, Yang WN, Jin H, Ma KG, Feng GF. Puerarin attenuates learning and memory impairments and inhibits oxidative stress in STZ-induced SAD mice. *Neurotoxicology.* 2015; 51:166–171. [PubMed: 26511841]
36. Black JE, Isaacs KR, Greenough WT. Usual vs. successful aging: Some notes on experiential factors. *Neurobiol Aging.* 1991; 12:325–328. [PubMed: 1961360]
37. Cho JY, Um HS, Kang EB, Cho IH, Kim CH, Cho JS, Hwang DY. The combination of exercise training and alpha-lipoic acid treatment has therapeutic effects on the pathogenic phenotypes of Alzheimer's disease in NSE/APPSw-transgenic mice. *Int J Mol Med.* 2010; 25:337–346. [PubMed: 20127037]
38. Swain RA, Harris AB, Wiener EC, Dutka MV, Morris HD, Theien BE, Konda S, Engberg K, Lauterbur PC, Greenough WT. Prolonged exercise induces angiogenesis and increases cerebral blood volume in primary motor cortex of the rat. *Neuroscience.* 2003; 117:1037–1046. [PubMed: 12654355]
39. Um HS, Kang EB, Koo JH, Kim HT, Jin-Lee, Kim EJ, Yang CH, An GY, Cho IH, Cho JY. Treadmill exercise represses neuronal cell death in an aged transgenic mouse model of Alzheimer's disease. *Neurosci Res.* 2011; 69:161–173. [PubMed: 20969897]
40. Trejo JL, Carro E, Torres-Aleman I. Circulating insulin-like growth factor I mediates exercise-induced increases in the number of new neurons in the adult hippocampus. *J Neurosci.* 2001; 21:1628–1634. [PubMed: 11222653]
41. Choi DH, Kwon IS, Koo JH, Jang YC, Kang EB, Byun JE, Um HS, Park HS, Yeom DC, Cho IH, Cho JY. The effect of treadmill exercise on inflammatory responses in rat model of streptozotocin-induced experimental dementia of Alzheimer's type. *J Exerc Nutrition Biochem.* 2014; 18:225–233.
42. Kang EB, Cho JY. Effects of treadmill exercise on brain insulin signaling and  $\beta$ -amyloid in intracerebroventricular streptozotocin induced-memory impairment in rats. *J Exerc Nutrition Biochem.* 2014; 18:89–96.

43. Zhang QG, Raz L, Wang R, Han D, De Sevilla L, Yang F, Vadlamudi RK, Brann DW. Estrogen attenuates ischemic oxidative damage via an estrogen receptor alpha-mediated inhibition of NADPH oxidase activation. *J Neurosci*. 2009; 29:13823–13836. [PubMed: 19889994]
44. Zhang QG, Wang R, Khan M, Mahesh V, Brann DW. Role of Dickkopf-1, an antagonist of the Wnt/beta-catenin signaling pathway, in estrogen-induced neuroprotection and attenuation of tau phosphorylation. *J Neurosci*. 2008; 28:8430–8441. [PubMed: 18716201]
45. Han D, Scott EL, Dong Y, Raz L, Wang R, Zhang Q. Attenuation of mitochondrial and nuclear p38 $\alpha$  signaling: A novel mechanism of estrogen neuroprotection in cerebral ischemia. *Mol Cell Endocrinol*. 2015; 400:21–31. [PubMed: 25462588]
46. Lu Q, Tucker D, Dong Y, Zhao N, Zhang Q. Neuro-protective and functional improvement effects of methylene blue in global cerebral ischemia. *Mol Neurobiol*. 2016; 53:5344–5355. [PubMed: 26433378]
47. Gan SD, Patel KR. Enzyme immunoassay and enzyme-linked immunosorbent assay. *J Invest Dermatol*. 2013; 133:e12. [PubMed: 23949770]
48. Barnes CA, Jung MW, McNaughton BL, Korol DL, Andreasson K, Worley PF. LTP saturation and spatial learning disruption: Effects of task variables and saturation levels. *J Neurosci*. 1994; 14:5793–5806. [PubMed: 7931545]
49. Cohen RM, Rezai-Zadeh K, Weitz TM, Rentsendorj A, Gate D, Spivak I, Bholat Y, Vasilevko V, Glabe CG, Breunig JJ, Rakic P, Davtayan H, Agadjanyan MG, Kepe V, Barrio JR, Bannykh S, Szekely CA, Pechnick RN, Town T. A transgenic Alzheimer rat with plaques, tau pathology, behavioral impairment, oligomeric A $\beta$ , and frank neuronal loss. *J Neurosci*. 2013; 33:6245–6256. [PubMed: 23575824]
50. Nagata K, Nakashima-Kamimura N, Mikami T, Ohsawa I, Ohta S. Consumption of molecular hydrogen prevents the stress-induced impairments in hippocampus-dependent learning tasks during chronic physical restraint in mice. *Neuropsychopharmacology*. 2009; 34:501–508. [PubMed: 18563058]
51. Wan H, Aggleton JP, Brown MW. Different contributions of the hippocampus and perirhinal cortex to recognition memory. *J Neurosci*. 1999; 19:1142–1148. [PubMed: 9920675]
52. Nunomura A, Perry G, Aliev G, Hirai K, Takeda A, Balraj EK, Jones PK, Ghanbari H, Wataya T, Shimohama S, Chiba S, Atwood CS, Petersen RB, Smith MA. Oxidative damage is the earliest event in Alzheimer disease. *J Neuropathol Exp Neurol*. 2001; 60:759–767. [PubMed: 11487050]
53. Choi DY, Lee YJ, Hong JT, Lee HJ. Antioxidant properties of natural polyphenols and their therapeutic potentials for Alzheimer's disease. *Brain Res Bull*. 2012; 87:144–153. [PubMed: 22155297]
54. Keller JN, Kindy MS, Holtsberg FW, St Clair DK, Yen HC, Germeyer A, Steiner SM, Bruce-Keller AJ, Hutchins JB, Mattson MP. Mitochondrial manganese superoxide dismutase prevents neural apoptosis and reduces ischemic brain injury: Suppression of peroxynitrite production, lipid peroxidation, and mitochondrial dysfunction. *J Neurosci*. 1998; 18:687–697. [PubMed: 9425011]
55. Zhang F, Jiang L. Neuroinflammation in Alzheimer's disease. *Neuropsychiatr Dis Treat*. 2015; 11:243–256. [PubMed: 25673992]
56. Serrano-Pozo A, Frosch MP, Masliah E, Hyman BT. Neuropathological alterations in Alzheimer disease. *Cold Spring Harb Perspect Med*. 2011; 1:a006189. [PubMed: 22229116]
57. Hardy J, Allsop D. Amyloid deposition as the central event in the aetiology of Alzheimer's disease. *Trends Pharmacol Sci*. 1991; 12:383–388. [PubMed: 1763432]
58. Rozemuller JM, Eikelenboom P, Stam FC, Beyreuther K, Masters CL. A4 protein in Alzheimer's disease: Primary and secondary cellular events in extracellular amyloid deposition. *J Neuropathol Exp Neurol*. 1989; 48:674–691. [PubMed: 2677252]
59. Petrov D, Pedrós I, Artiach G, Sureda FX, Barroso E, Pallàs M, Casadesús G, Beas-Zarate C, Carro E, Ferrer I, Vazquez-Carrera M, Folch J, Camins A. High-fat diet-induced deregulation of hippocampal insulin signaling and mitochondrial homeostasis deficiencies contribute to Alzheimer disease pathology in rodents. *Biochim Biophys Acta*. 2015; 1852:1687–1699. [PubMed: 26003667]

60. Liu HL, Zhao G, Zhang H, Shi LD. Long-term treadmill exercise inhibits the progression of Alzheimer's disease-like neuropathology in the hippocampus of APP/PS1 transgenic mice. *Behav Brain Res.* 2013; 256:261–272. [PubMed: 23968591]
61. Selkoe DJ. Alzheimer's disease: Genes, proteins, and therapy. *Physiol Rev.* 2001; 81:741–766. [PubMed: 11274343]
62. Correia SC, Santos RX, Santos MS, Casadesus G, Lamanna JC, Perry G, Smith MA, Moreira PI. Mitochondrial abnormalities in a streptozotocin-induced rat model of sporadic Alzheimer's disease. *Curr Alzheimer Res.* 2013; 10:406–419. [PubMed: 23061885]
63. Heneka MT, O'Banion MK. Inflammatory processes in Alzheimer's disease. *J Neuroimmunol.* 2007; 184:69–91. [PubMed: 17222916]
64. Zhu D, Yang N, Liu YY, Zheng J, Ji C, Zuo PP. M2 macrophage transplantation ameliorates cognitive dysfunction in amyloid- $\beta$ -treated rats through regulation of microglial polarization. *J Alzheimers Dis.* 2016; 52:483–495. [PubMed: 27003214]
65. De Felice FG, Ferreira ST. Inflammation, defective insulin signaling, and mitochondrial dysfunction as common molecular denominators connecting type 2 diabetes to Alzheimer disease. *Diabetes.* 2014; 63:2262–2272. [PubMed: 24931033]
66. Witte ME, Geurts JJ, de Vries HE, van der Valk P, van Horsen J. Mitochondrial dysfunction: A potential link between neuroinflammation and neurodegeneration? *Mitochondrion.* 2010; 10:411–418. [PubMed: 20573557]
67. Urrutia PJ, Mena NP, Núñez MT. The interplay between iron accumulation, mitochondrial dysfunction, and inflammation during the execution step of neurodegenerative disorders. *Front Pharmacol.* 2014; 5:38. [PubMed: 24653700]
68. Wang X, Wang W, Li L, Perry G, Lee HG, Zhu X. Oxidative stress and mitochondrial dysfunction in Alzheimer's disease. *Biochim Biophys Acta.* 2014; 1842:1240–1247. [PubMed: 24189435]
69. Yamane T, Ikari Y, Nishio T, Ishii K, Ishii K, Kato T, Ito K, Silverman DH, Senda M, Asada T, Arai H, Sugishita M, Iwatsubo T. Study J-ADNI, Group. Visual-statistical interpretation of (18)F-FDG-PET images for characteristic Alzheimer patterns in a multicenter study: Inter-rater concordance and relationship to automated quantitative evaluation. *AJNR Am J Neuroradiol.* 2014; 35:244–249. [PubMed: 23907243]
70. Shokouhi S, Claassen D, Kang H, Ding Z, Rogers B, Mishra A, Riddle WR. Alzheimer's Disease Neuroimaging Initiative. Longitudinal progression of cognitive decline correlates with changes in the spatial pattern of brain 18F-FDG PET. *J Nucl Med.* 2013; 54:1564–1569. [PubMed: 23864720]
71. Landau SM, Harvey D, Madison CM, Koeppe RA, Reiman EM, Foster NL, Weiner MW, Jagust WJ. Alzheimer's Disease Neuroimaging Initiative. Associations between cognitive, functional, and FDG-PET measures of decline in AD and MCI. *Neurobiol Aging.* 2011; 32:1207–1218. [PubMed: 19660834]
72. Terni B, Boada J, Portero-Otin M, Pamplona R, Ferrer I. Mitochondrial ATP-synthase in the entorhinal cortex is a target of oxidative stress at stages I/II of Alzheimer's disease pathology. *Brain Pathol.* 2010; 20:222–233. [PubMed: 19298596]
73. Pettegrew JW, Panchalingam K, Klunk WE, McClure RJ, Muenz LR. Alterations of cerebral metabolism in probable Alzheimer's disease: A preliminary study. *Neurobiol Aging.* 1994; 15:117–132. [PubMed: 8159258]
74. Price JL, McKeel DW Jr, Buckles VD, Roe CM, Xiong C, Grundman M, Hansen LA, Petersen RC, Parisi JE, Dickson DW, Smith CD, Davis DG, Schmitt FA, Markesbery WR, Kaye J, Kurlan R, Hulette C, Kurland BF, Higdon R, Kukull W, Morris JC. Neuropathology of nondemented aging: Presumptive evidence for preclinical Alzheimer disease. *Neurobiol Aging.* 2009; 30:1026–1036. [PubMed: 19376612]

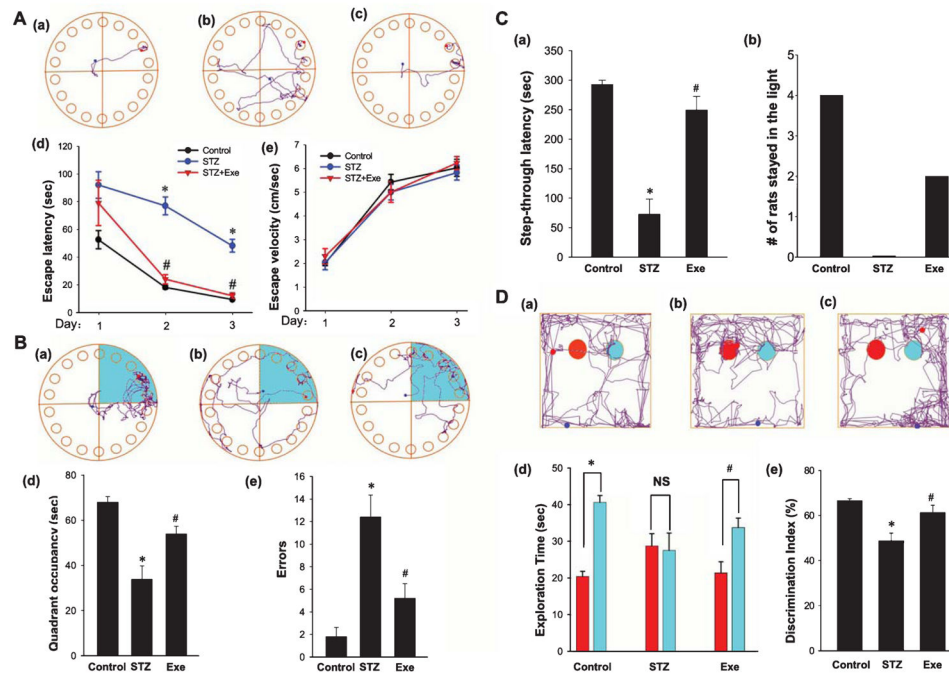


**Fig. 1.** Effect of treadmill exercise on STZ-induced spatial learning and memory deficits in rats. A) Representative tracking plots of Barnes Maze test for the indicated rats on the third trial day: (a) Control, (b) STZ, (c) STZ + Exe. Escape latencies and the average velocity were recorded and statistical data are shown in (d and e). B) Tracking plots and occupancy in target quadrant (green color) were recorded on probe day 4. (a)–(c) indicate the typical tracking plots for control, STZ, and STZ + Exe, respectively. Relative quadrant occupancy and errors made during Barnes Maze testing were recorded and statistically analyzed (d and e). C) The step-through latency (a) and numbers of rats that stayed in the bright chamber over 300 s (b) are shown in the passive avoidance test. D) Five-min novel object recognition tests were subsequently performed to compare the recognition memory. Representative traces are displayed for rat exploration of the familiar object (red) and a novel object (Cyan) (a: control, b: STZ, c: STZ + Exe). Diagram analysis of exploration time for different objects (d) and discrimination index (e) are indicated.  $n = 8$  per group. \* $p < 0.05$  versus normal control; # $p < 0.05$  versus STZ group.

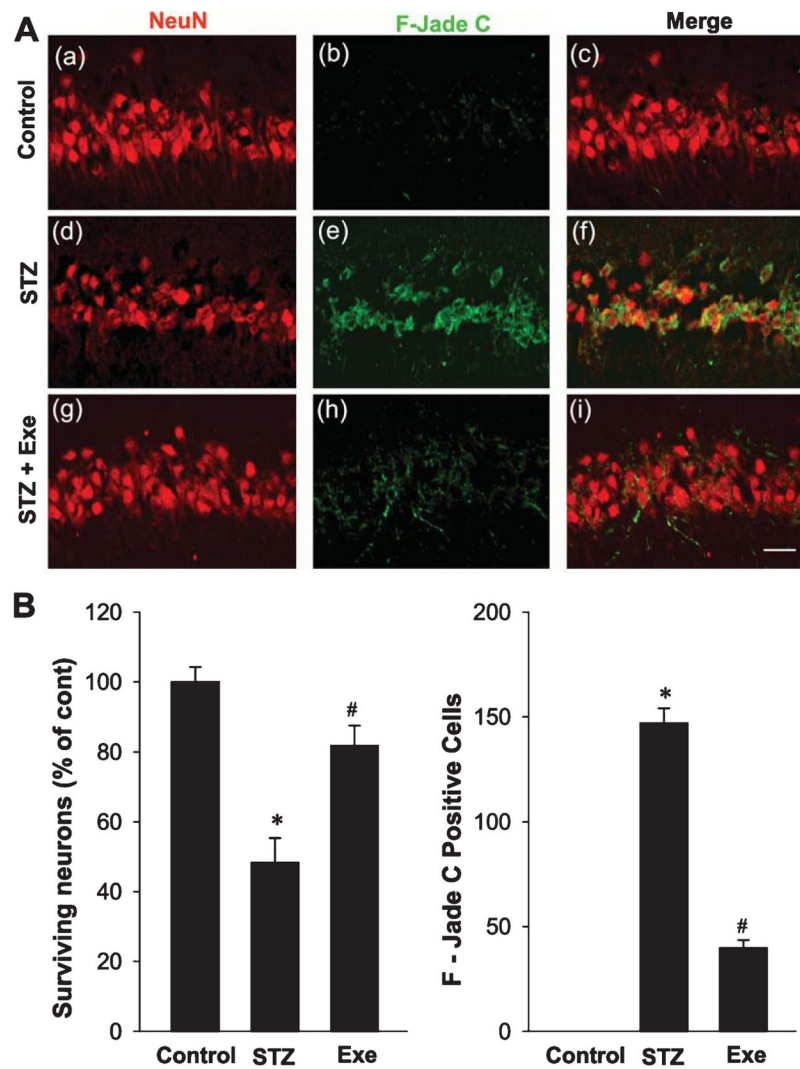


**Fig. 2.** Effect of treadmill exercise on STZ-induced hippocampal neuronal degeneration. A) Representative confocal pictures of rat hippocampal pyramidal CA1 neurons from control, STZ, STZ + Exe groups stained with the neuronal marker, NeuN and the neurodegenerative marker, F-Jade C, indicating robust neuron loss and neuronal degeneration following STZ insult, which was significantly attenuated by treadmill exercise. Scale bar = 20  $\mu$ m. B) Quantification analysis was performed by counting surviving neurons and F-Jade C-positive neurons. The results indicate that neuronal loss and acute neuronal degeneration were induced by STZ administration at early stage of AD progression, whereas treadmill exercise exerted significant neuroprotection by increasing neuronal survival and decreasing neurodegeneration.  $n = 8$  per group. Values are means  $\pm$  SE. \* $p < 0.05$  versus normal control; # $p < 0.05$  versus STZ group.



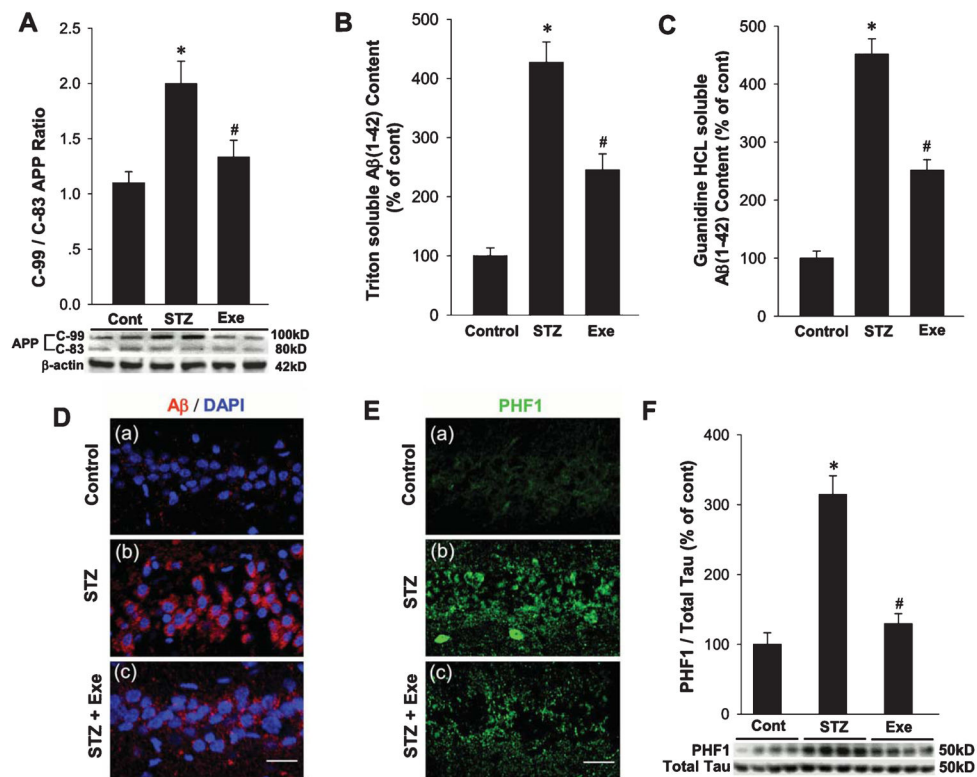


**Fig. 3.** Effects of treadmill exercise on STZ-induced amyloidogenic processing of AβPP, Aβ accumulation, and tau phosphorylation in rat hippocampal CA1 region. A) Western blot analysis for C-terminal fragment of AβPP after α-secretase cleavage (C-83) and β-secretase cleavage (C-99), and the quantification analysis of C-99 to C-83 fragments ratios. B,C) The levels of Triton soluble Aβ<sub>1-42</sub> and Guanidine HCL soluble Aβ<sub>1-42</sub> were analyzed, and the data were expressed as fold changes versus control group. D) Representative Aβ<sub>1-42</sub> staining for control, STZ, and STZ + Exe groups in hippocampal CA1 region. Scale bar = 20 μm. E, F) Phosphorylation of tau protein (PHF) was examined by immunofluorescent staining and western blot analysis, respectively. Scale bar = 20 μm. *n* = 5 per group. Values are means ± SE. \**p* < 0.05 versus normal control; #*p* < 0.05 versus STZ group.



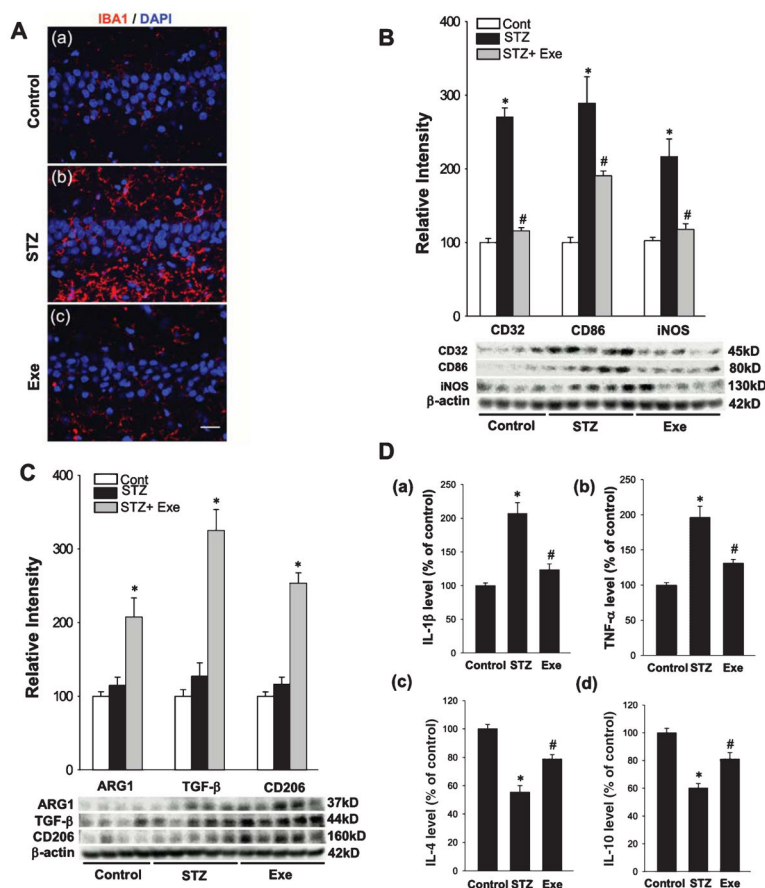


**Fig. 4.** Treadmill exercise shifts microglial polarization from M1 to M2 phenotype and suppresses pro-inflammatory cytokines production. A) Confocal analysis of hippocampal CA1 neurons immunostained for IBA1, a marker of microglia. As shown above, STZ enhanced microglia activation and this effect was markedly suppressed by treadmill exercise. B, C) Western blot analysis for M1 and M2 markers of activated microglial revealed that treadmill exercise shifted activated microglia to M2 phenotype, while M1 phenotype was significantly inhibited. D) Levels of representative pro-inflammatory (a) & (b) and anti-inflammatory cytokines (c) & (d) were detected. Consistent with microglial polarization, treadmill exercise reversed STZ-induced elevation of pro-inflammatory cytokines and decrease of anti-inflammatory cytokines. Scale bar = 20  $\mu$ m.  $n = 5$  per group. \* $p < 0.05$  versus normal control; # $p < 0.05$  versus STZ group.

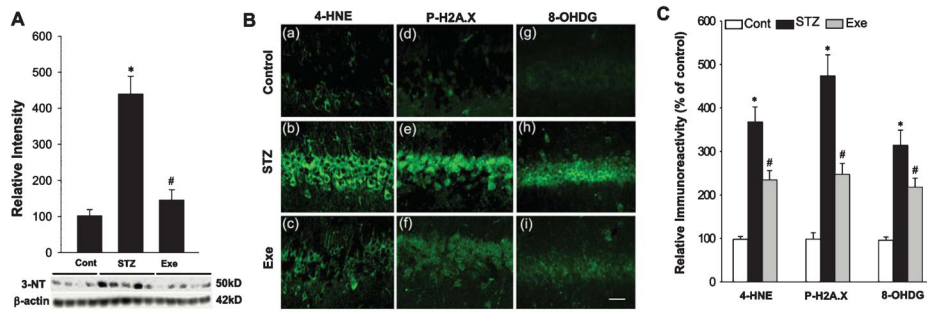


**Fig. 5.** Treadmill exercise ameliorates STZ-induced oxidative stress damage. A) Western blot analysis of reactive nitrogen species (RNS) generation, marked by 3-NT. STZ-induced RNS accumulation was markedly attenuated by treadmill exercise during AD progression. B) Confocal analysis for oxidative stress-induced damage to basic cellular components: lipid, histone and DNA, marked by 4-HNE (a–c), P-H2A.X (d–f), and 8-OHDG (g–i) respectively. Note that treadmill exercise significantly attenuated STZ-induced cellular oxidative damages. C) Relative immunoreactivity was analyzed in a diagram form following the confocal analysis above, with data expressed as fold changes versus normal control. Scale bar = 20  $\mu$ m.  $n = 5$  per group. Values are means  $\pm$  SE. \* $p < 0.05$  versus normal control; # $p < 0.05$  versus STZ group.

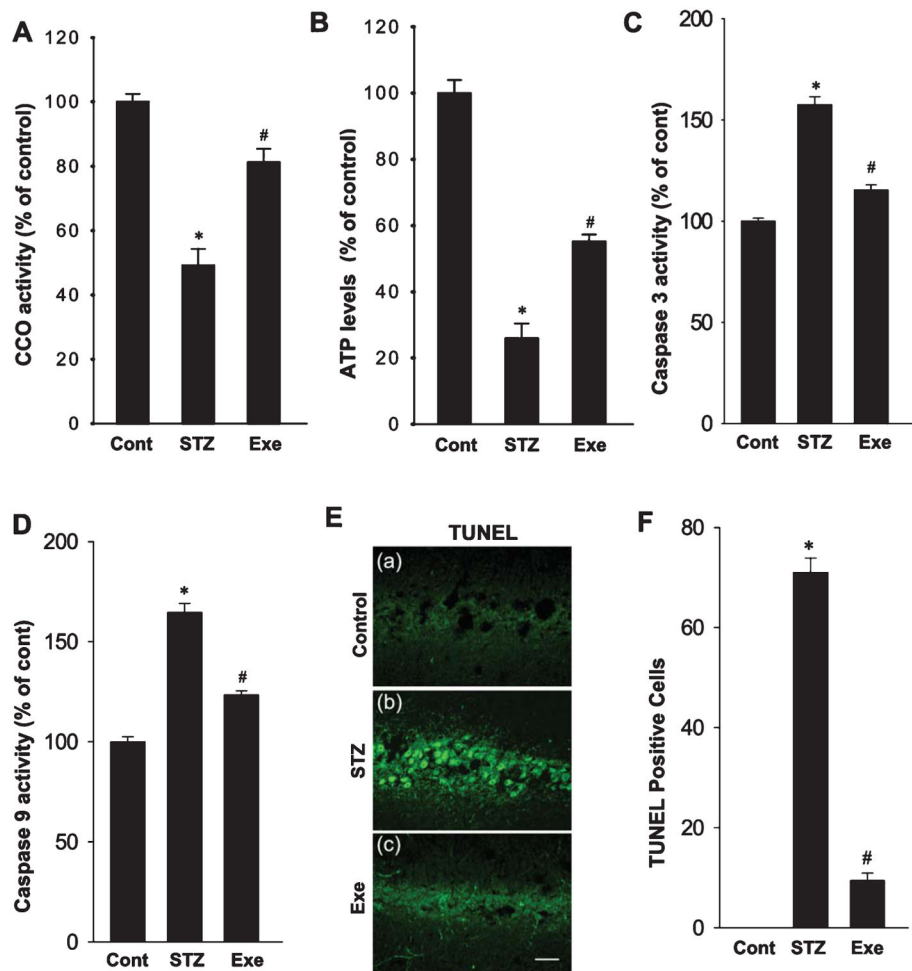


**Fig. 6.** Treadmill exercise attenuates STZ-induced mitochondrial dysfunction and the consequent activation of caspase-9/caspase-3 apoptotic pathway. A, B) ELISA analysis of mitochondrial cytochrome c oxidase activity followed by the total ATP production were performed to examine mitochondrial oxidative phosphorylation level. C, D) The activities of pro-apoptotic proteins caspase 3/9 were subsequently analyzed, revealing that the enhanced activations of these pro-apoptotic proteins were inhibited by treadmill exercise. E) Representative confocal images of TUNEL staining revealed aggravated neuron apoptosis following dramatic mitochondrial dysfunction. F) TUNEL-positive cells per 250  $\mu\text{m}$  in each confocal image were counted and expressed in graphic depiction. Values are means  $\pm$  SE. Scale bar = 20  $\mu\text{m}$ .  $n = 5$  per group. \* $p < 0.05$  versus normal control; # $p < 0.05$  versus STZ group.